

EXECUTIVE SUMMARY

LTX- β has successfully completed the first part of the FES Notable Outcome for FY2020 due on January 31, 2020. The FES Notable Outcome is restated here:

Complete the first kinetically constrained equilibrium reconstructions of neutral beam heated/fueled LTX- β plasmas with fully coated solid and liquid lithium walls. Using these equilibria, estimate the energy confinement time of low-recycling LTX- β plasmas and submit a report documenting the finding by January 31, 2020. Beyond submitting a report to DOE, disseminate these energy confinement findings at a major fusion-relevant scientific conference by September 30, 2020 (Objective 1.1).

LTX- β has been operated with a full suite of kinetic diagnostics, including Thomson scattering and active CHERS. Data from Thomson scattering and CHERS has been used to constrain equilibrium reconstructions with both solid and liquid lithium wall coatings, and produce estimates of the energy confinement time during neutral beam heating. The submission of this report thus fulfills the requirements of the DOE notable outcome cited above, which are due by January 31, 2020. In addition, the LTX- β team will report on these findings at the 24th International Conference on Plasma-Surface interactions in Korea, May 31 – June 5, 2020, and plans to report results at the 47th European Physical Society Conference on Plasma Physics in Spain, June 22 – 26, 2020. Both conferences are major fusion-relevant scientific conferences, to fulfill the final requirement for this notable outcome.

INTRODUCTION

The major research goal for the LTX- β group in FY2020 is to document plasma energy confinement as the global recycling is varied over a wide range through the use of lithium plasma-facing surfaces. In order to adequately document energy confinement in a low aspect ratio tokamak, equilibrium reconstructions which are constrained by Thomson scattering temperature and density profiles are required. Measurements of the core ion temperature with charge-exchange recombination spectroscopy (CHERS) are another valuable constraint. Although all major systems for LTX- β had been in place, and the tokamak operated at increased toroidal field (>3 kG), with up to 600 kW of neutral beam injection by the end of March 2019, the Thomson scattering diagnostic had not been completely installed, and the 30+ year old legacy laser required significant maintenance. Several facility improvements were required to enable the confinement time estimates and are summarized here:

- The increased toroidal field at which LTX- β operates, compared to LTX, mandated additional mechanical stabilization of the viewing lens and fiber collection bundle, as well as redesign of the exit beamline and laser dump.
- The neutral beam provided by Tri-Alpha Energy was not designed for diagnostic purposes, and required significant upgrades to improve reproducibility, and reduce the significant variation of beam current throughout the pulse in order to enable reliable CHERS measurements.
- In FY2019 a simplified lithium evaporation system had been installed, which, although capable of completely coating the plasma-facing surfaces, was not optimized to preferentially coat the primary area of plasma contact, the high field-side heated “shells” – the segmented stainless steel, copper-backed liner in LTX- β . During FY2020 the lithium evaporators have been upgraded to increase high field side deposition.

- Numerous other systems, such as Langmuir probes to determine the edge density and temperature which are required to characterize recycling were not operational during FY2019. In FY2020 these diagnostics have been commissioned.

Very recently, plasma current in LTX-β has been increased to 100 kA, although the discharges analyzed for this report operated with plasma current in the 55 – 75 kA range. Peak electron temperature in the recent, higher current discharges was seen to exceed 200 eV.

FACILITY IMPROVEMENTS

Thomson scattering

A photograph of LTX-β showing the Thomson scattering laser beamline and the support for the viewing optics is shown in Figure 1. LTX-β is located on the second floor of the small experiments laboratory building at PPPL, and during a discharge the Thomson viewing system was found to be displaced due to motion of the floor and magnetic forces on the lens support structure. Additional overhead bracing, and bracing from the machine support structure, had to be installed to stabilize the system. Figure 2 shows the beamline exit area. The input and exit windows are placed away from the focus, at locations where the laser power density is safely below the damage threshold. The original (LTX) blue glass laser dump location on the exit beamline physically interfered with the neutral beam dump tank, and required an additional in-vacuum mirror to redirect the beam dump. The exit window and the laser dump are now located near the room ceiling.

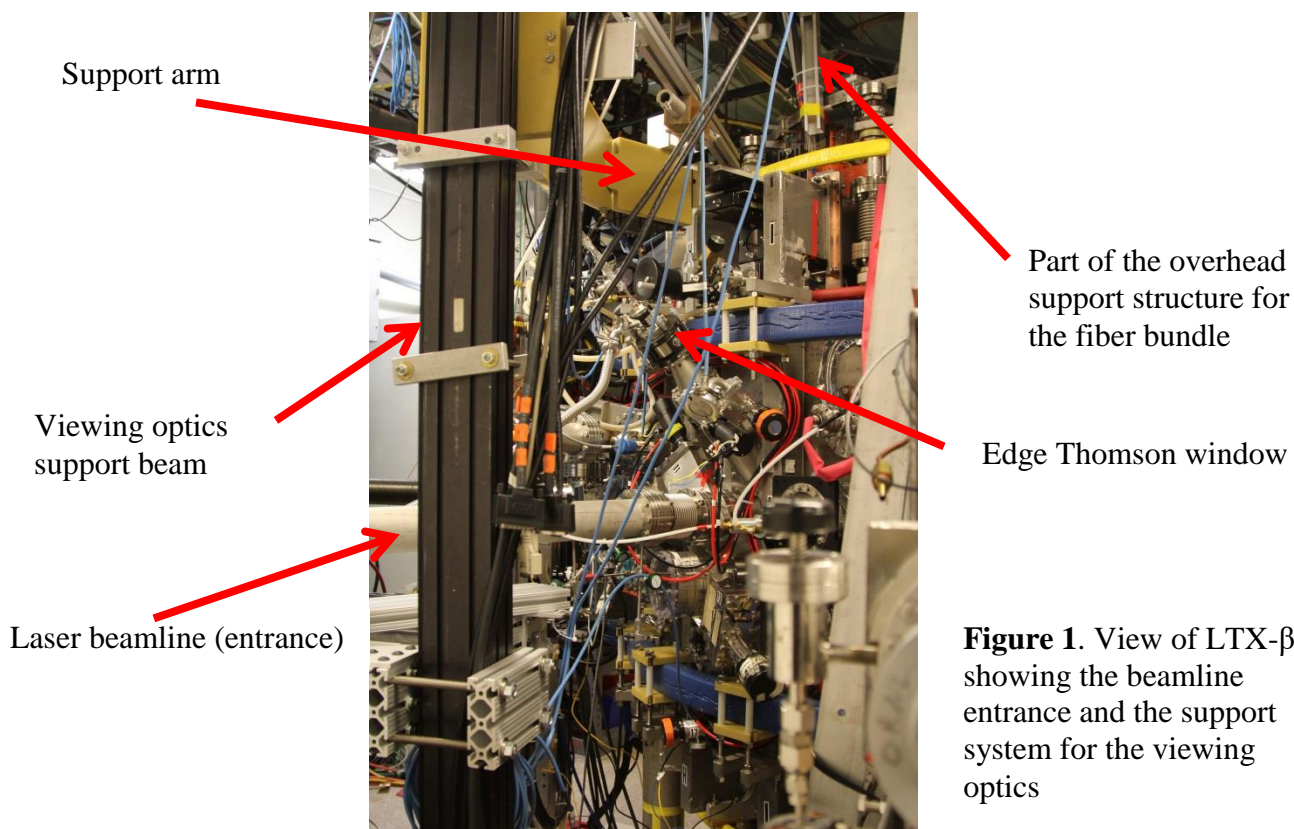


Figure 1. View of LTX-β showing the beamline entrance and the support system for the viewing optics

Figure 1. View of LTX-β from the north. The main pump duct is to the right and the Thomson scattering laser (black enclosure) is to the left, in this view.

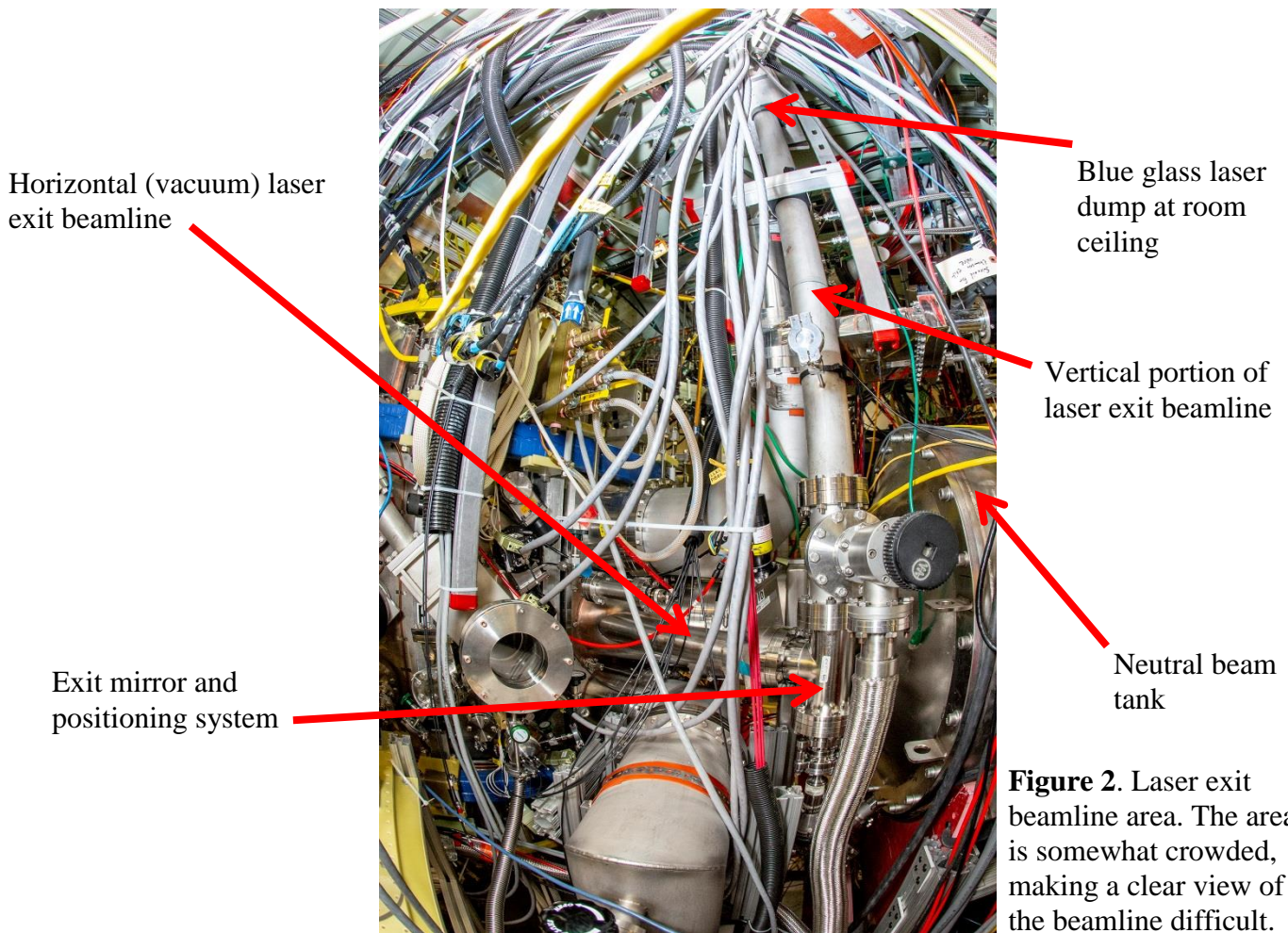


Figure 2. Laser exit beamline area. The area is somewhat crowded, making a clear view of the beamline difficult.

Neutral beam

We have made substantial progress on improving the operation of the neutral beam, on loan from Tri Alpha Energy Technologies, which is both the auxiliary heating source and the diagnostic beam for LTX- β . Figure 3 shows the evolution of the ion source (arc), neutral beam current and voltage, and beam power and perveance for a beam pulse dating from September 2019 (dashed lines) before improvements were made to the original Russian system. The strong evolution of the beam current, power, and perveance, as well the shot-to-shot irreproducibility of the beam, made the pulse poorly suited for use with a CHERS diagnostic. While still useful for heating, the drop in injected power by the end of the beam pulse clearly limited the injected energy.

Accordingly, several of the power supplies powering the beam arc (the plasma source used for ion extraction) were scrapped and rebuilt. All the fast gas valves used in the beam source were replaced with highly reproducible fast gas valves supplied by the Parker-Hannifin Co., and new valve driver circuits were designed, built, and installed. This substantial rebuild of the neutral beam system resulted in a significant improvement in the beam pulse behavior – current and voltage traces with the upgraded system are also shown in Figure 3 (solid lines).

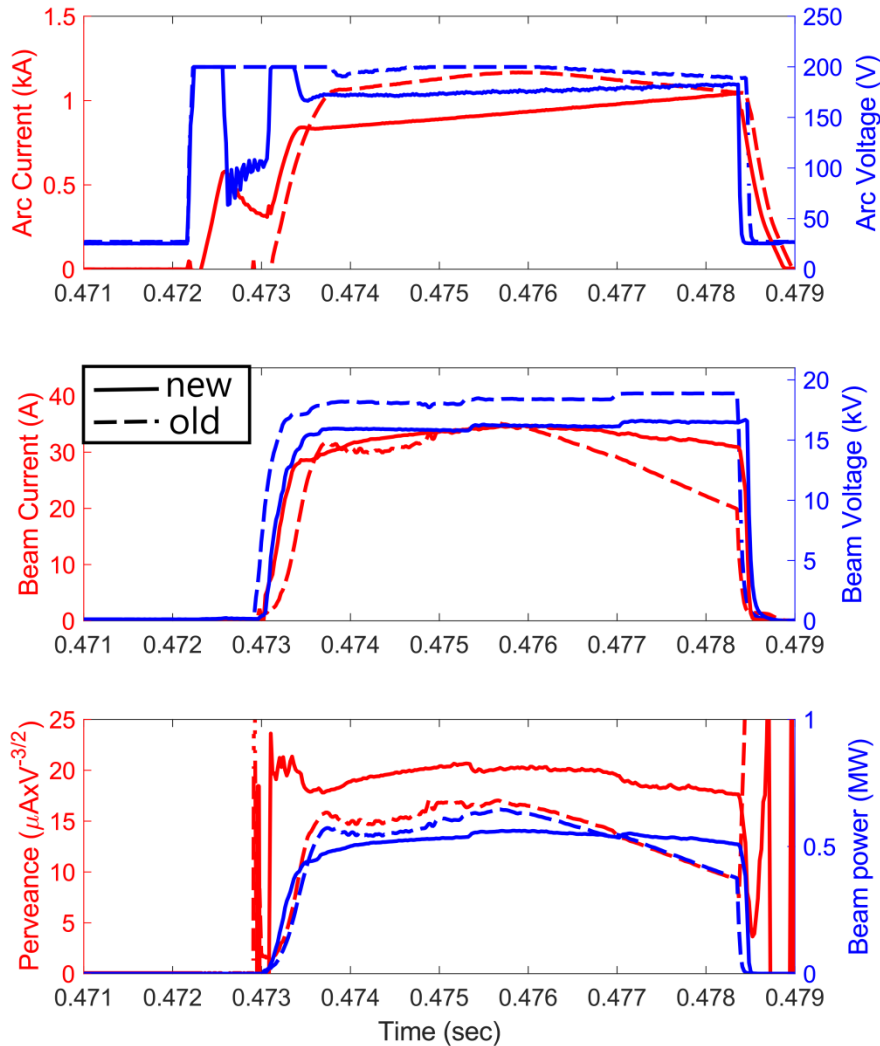


Figure 3. Dashed lines: neutral beam behavior during September 2019 LTX- β operations, before the Russian beam power supplies were partially rebuilt. Note the strong sag in the beam current, as well as the beam power and perveance. Solid lines: neutral beam behavior during recent LTX- β operations (January 2020).

Beam divergence has also been reduced, and the beam can now operate at high injected current, even with reduced voltage. In Figure 4 a scan of the neutral beam perveance, and the resulting divergence scan, during measurements with the PPPL high-throughput accurate-wavelength lens-based (HAL) visible spectrometer system, viewing the beam through the ORNL CHERS optics.

Low divergence is required in order to increase the beam density and therefore the charge-exchange signal for the active CHERS diagnostic, as well as the fraction of the neutral beam which passes through the modest vertical gap (14 cm) between the outboard upper and lower shells (liners) in LTX- β . At 0.02 radians >90% of the injected beam traverses the shell gap. The divergence reduction was primarily accomplished by carefully tuning the discharge current through the neutral beam's washer gun plasma source.

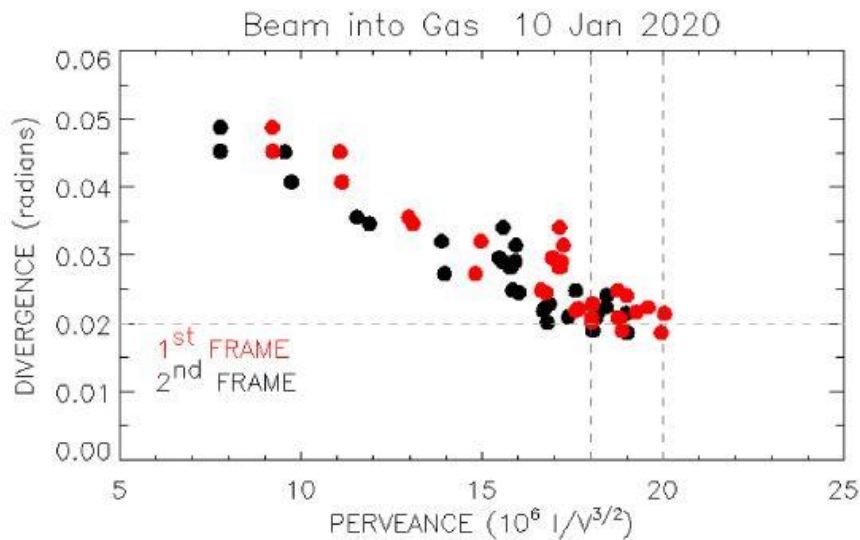


Figure 4. Perveance scan. The target perveance is 18-20, and the specified minimum divergence on the beam is 0.02 radians.

Beam-into-gas operation also produces results for the beam species mix (first, second, and third energy components, as well as the water impurity level). These results are shown in Figure 5.

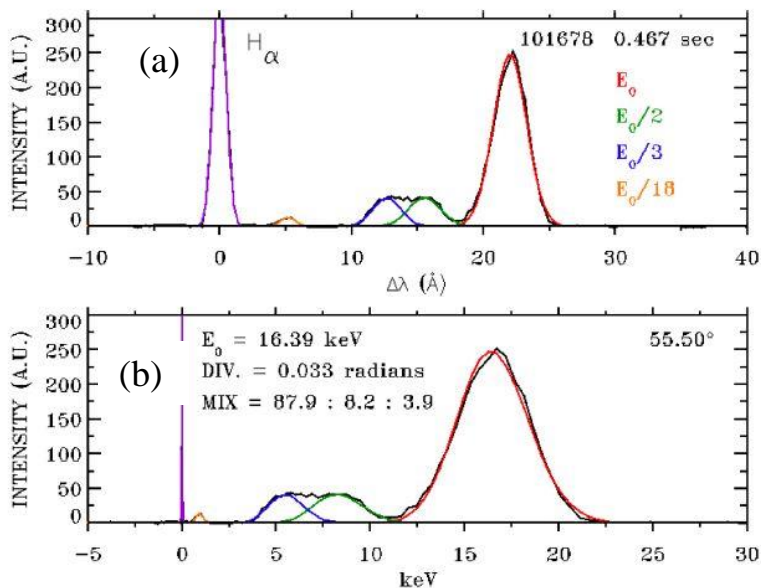


Figure 5. (a) Spectral intensity measured with HAL as a function of the deviation in wavelength from the H- α spectral line. Light from the full, half, and third energy components emitted by the neutral beam source can be seen. ~88% of the beam current is in the first energy component. Note the very small peak at $E_0/18$, which represents the residual water impurity. (b) Translation from Doppler shifted wavelength into energy.

Langmuir probes

An accurate determination of plate recycling at the primary plasma contact point – the high field side shell faces, which form the plasma limiting surface – requires a determination of the plasma density and electron temperature at the limiter, as well as a calibrated Lyman- α array, to provide input for DEGAS2. In LTX, we were unable to document the changes in the SOL temperature as neutral gas was pumped from the edge, and the electron temperature flattened, since the LTX Langmuir probe circuitry was borrowed from NSTX, and was designed for low electron temperatures. A set of robust, fixed high field side Langmuir probes designed to operate at high sweep voltages was installed during the upgrade to LTX- β , along with a moveable low field side (LFS) probe. A preliminary comparison of the behavior of the edge density and electron temperature for discharges with passivated lithium, and with fresh lithium, from the LFS probe, is shown in Figure 6. Note that the pre-deposition discharge

had a shorter duration than the post-lithium discharge (although the plasma density was approximately the same in both cases). For the post-lithium discharge, after gas puffing is terminated at $t=457$ msec, the edge electron temperature increases by 2-3 \times , after a short delay during which neutrals in the SOL are pumped by the lithium wall.

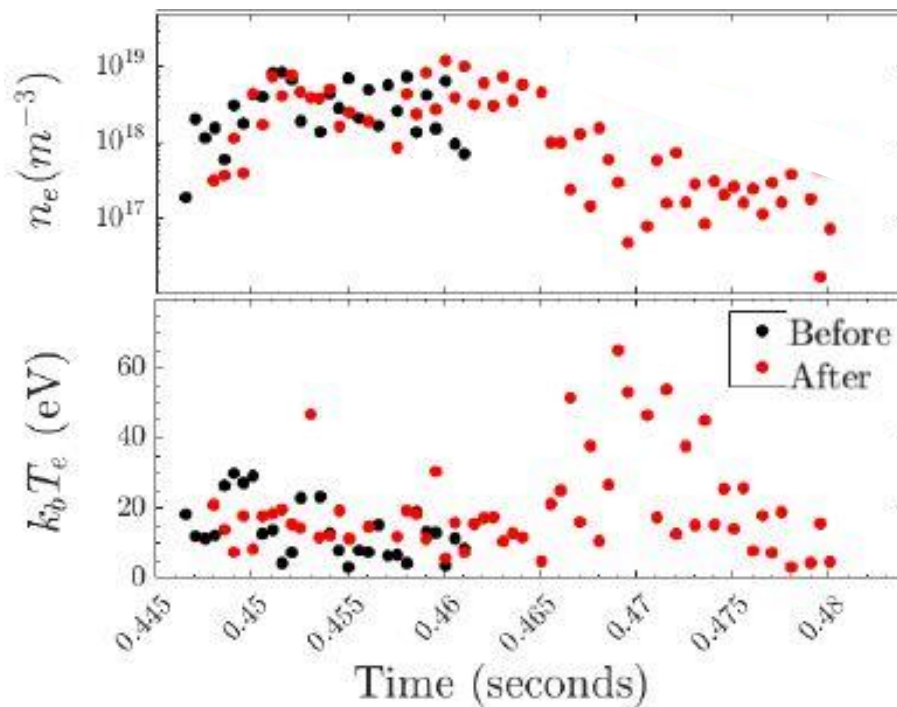


Figure 6. Edge electron density and temperature **Before** and **After** lithium deposition.

Lithium evaporators

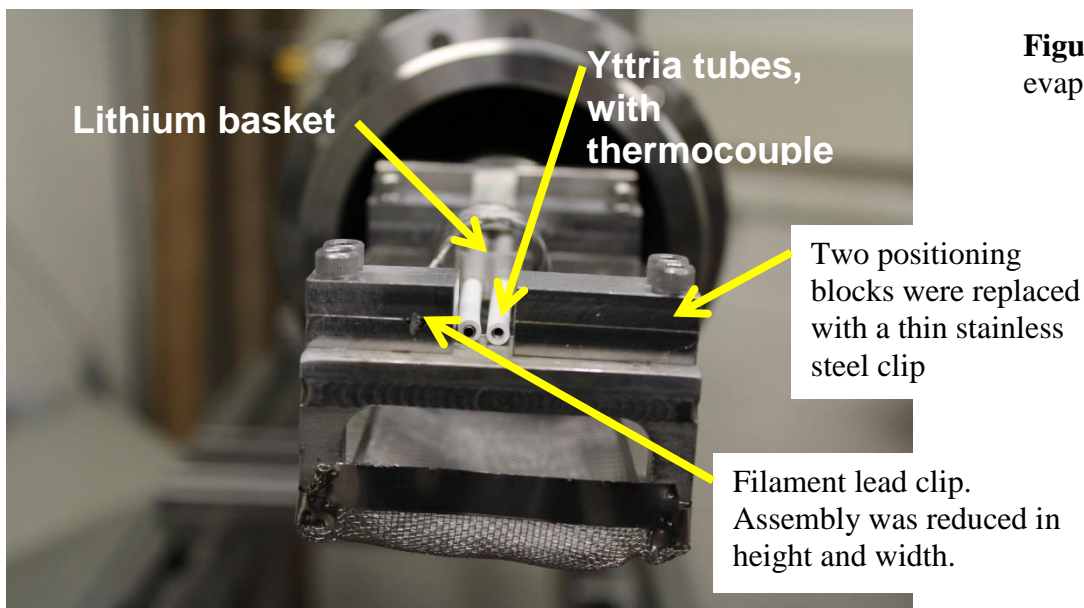


Figure 7. Lithium evaporator modifications.

The evaporators installed for the March 2019 run campaign were primarily designed to coat the plasma-facing surfaces using a small lithium inventory. However, modeling of the distribution of the coating indicated that the coating was thinnest on the high field side, where the plasma limits. The

evaporators were modified to increase the evaporated lithium flux to the high field side and reinstalled, although the geometry of the lithium inventory (thin horizontal sheets) continues to favor upward and downward evaporation. The modifications are indicated in Figure 7. A more complete redesign and rebuild of the evaporators, to increase the lithium inventory and further modify the evaporation pattern to preferentially coat the high field side surfaces is planned for February/March.

RESULTS

Profiles of T_e , n_e from Thomson Scattering

Electron temperature profiles have been determined via Thomson scattering for discharges with cold shells (solid lithium coated) and hot (200 °C), liquid lithium coated shells, during neutral beam injection. Profiles for operation with hot shells are shown in Figure 8. The neutral beam is injected from $t=463$ msec to $t=468$ msec. Since the Thomson scattering system laser system only provides a single laser pulse per discharge, a determination of the evolution of the electron temperature requires several discharges, while the laser firing time is stepped through the discharge. In addition, data from several discharges was averaged to produce the profiles.

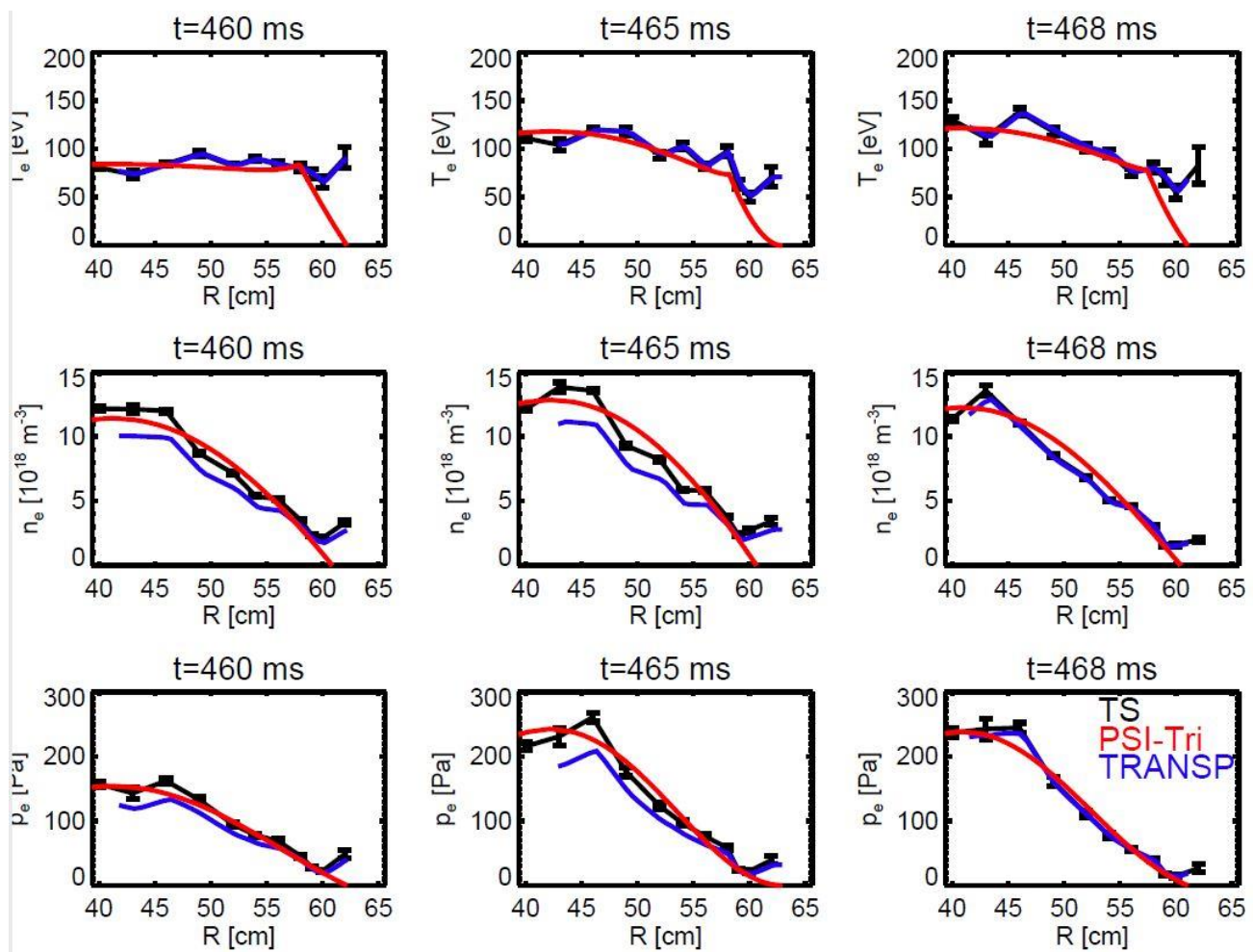


Figure 8. Electron temperature profiles just prior to beam injection ($t=460$ msec), during beam injection ($t=465$ msec), and at the end of the beam pulse ($t=469$ msec).

Plasma current during hot wall operation was limited to 50 – 60 kA, which is not sufficient to confine the fast beam ions. Consequently, a comparison of discharges with and without beam injection as yet shows little evidence of heating. Profiles from a hot wall discharge without beam injection are shown in Figure 9.

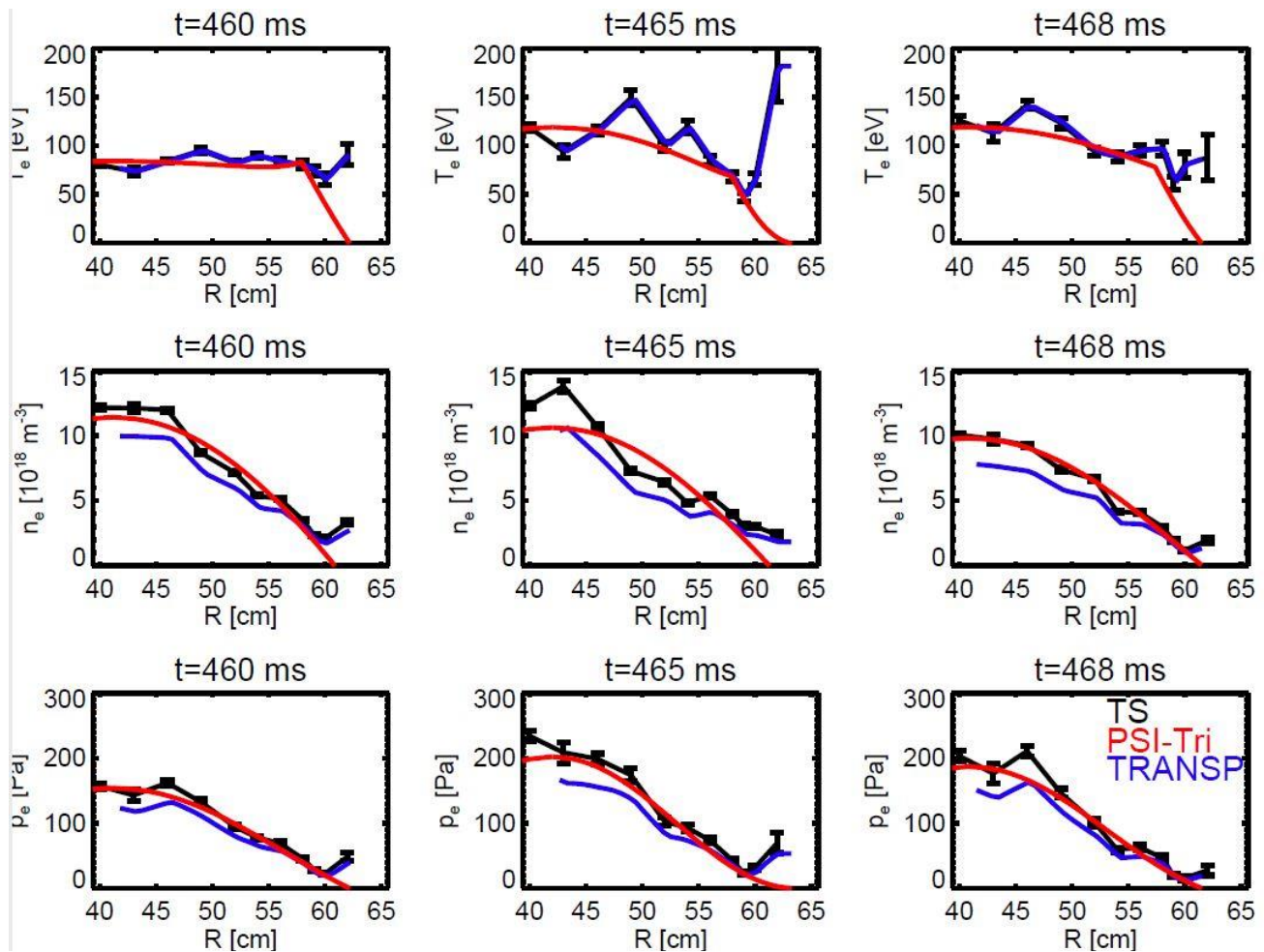


Figure 9. Electron temperature profiles without beam injection, for the same times in the discharge (460, 465, and 468 msec) shown in Figure 8.

There is still significant scatter in the Thomson scattering profiles, especially at lower density near the plasma edge. The temperature profiles are relatively flat, with peak temperatures in the 100 – 150 eV range, for discharges with either cold or hot walls, and plasma current in the 55 – 75 kA range.

Core ion temperature (CHERS)

This report presents the first data taken with active CHERS on LTX- β . Active CHERS is a unique capability for an experiment of the scale of LTX- β . All data reported here was taken with the HAL spectrometer, which was developed for use on NSTX-U, but is being used on LTX- β during NSTX-U recovery. HAL views the neutral beam through the ORNL-designed and fabricated CHERS viewing system. The ORNL CHERS diagnostic allows for the simultaneous acquisition of Doppler-shifted Li-III lines viewed within the beam cross section, as well as background spectra with an oppositely-directed set of views which do not intersect the beam path as shown in Figure 10.

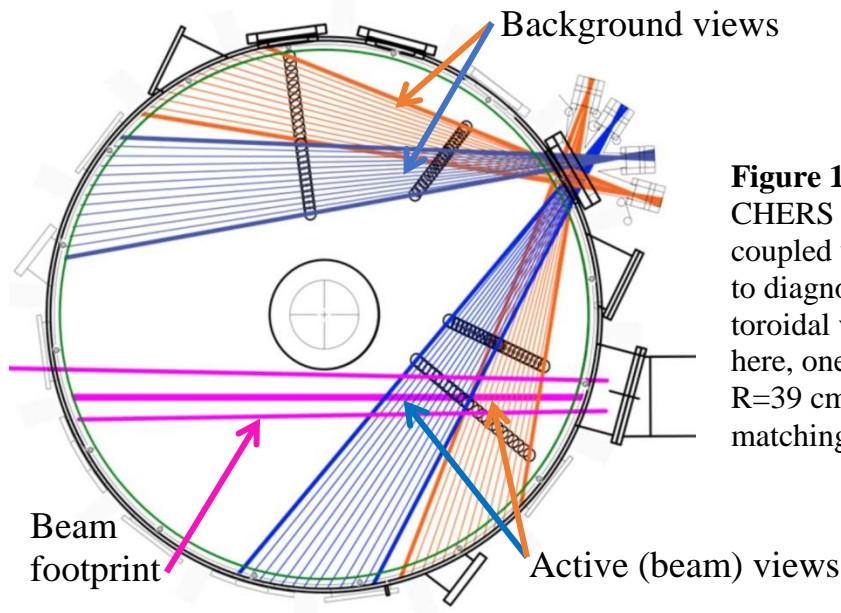


Figure 10. Viewing chords for the ORNL CHERS diagnostic, which employs fiber-coupled views input to the HAL spectrometer to diagnose ion temperature and plasma toroidal velocity. For the initial data shown here, one active chord (viewing the plasma at R=39 cm, just outboard of the axis) and the matching background chord were employed.

The CHERS data acquired by HAL is averaged over 2.5 msec windows; the first such window spans the first half of the beam injection window, and the second window spans the second half of the beam, as shown in Figure 11.

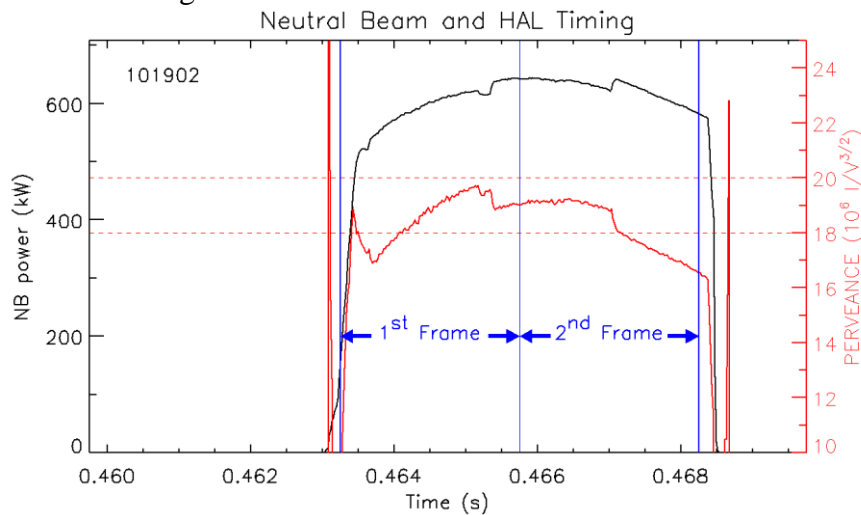


Figure 11. CHERS averaging windows for the neutral beam pulse

A comparison of the ion impurity (lithium) temperature and the toroidal velocity early and late in the beam pulse is shown in Figure 12. This discharge employed hot (liquid) lithium wall coatings at 200°C, and is part of the set of discharges shown in the Thomson scattering profiles shown in Figure 8. Again, the plasma current was relatively low for all the discharges with liquid walls, ~55 kA. The increase in ion temperature shown was the largest observed for hot shell operation, although the ion temperature measured during the first half of beam injection (30-40 eV) was similar to other discharges with liquid walls.

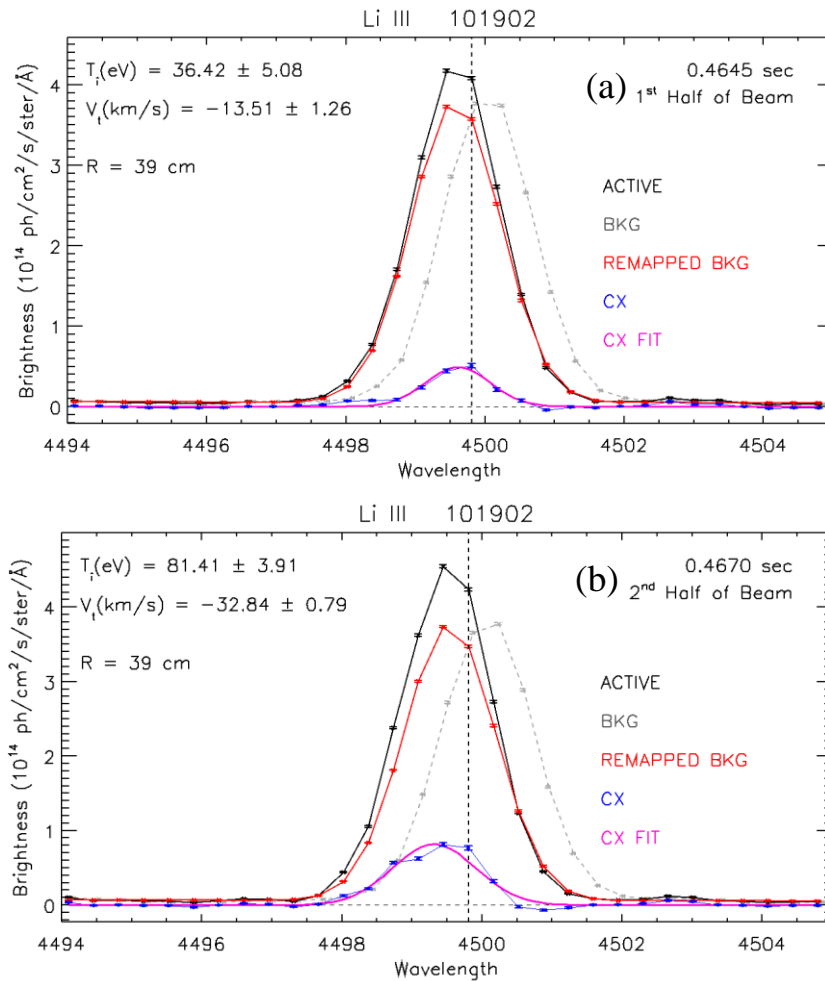


Figure 12. (a) Li III line width and shift for the first half of the beam injection pulse, and (b) for the second half of the beam pulse. Aside from a temperature increase from 36 to 81 eV during the pulse, the toroidal velocity increases from ~ 14 to 33 km/sec. This was the largest observed change in ion temperature during beam injection.

An increase in toroidal velocity is expected due to fast ion losses. Since the rotation velocity is opposite to the direction of beam injection, the observed rotation is not due to injection of toroidal momentum by the beam. Although there is evidence for some ion heating during beam injection on most of the discharges which have been analyzed, not every discharge shows a significant increase in ion temperature during beam injection. The increase in toroidal rotation also varies from discharge to discharge. Finally, TRANSP modeling would predict an increase in ion temperature even in the absence of beam injection, under the assumption that ion confinement is neoclassical.

Constrained equilibrium reconstructions

Equilibrium reconstructions have been performed with the University of Washington Psi-Tri code, constrained by the Thomson scattering data and the central ion temperature from CHERS. For the first (pre-beam) time at 460 msec, the ratio of T_i/T_e for the data at 465 msec was also assumed. Reconstructions for the hot shell discharges shown in Figure 8 and 9 are shown below, in Figure 13. There is a minor evolution in plasma shape as the discharge progresses. The constrained equilibrium reconstructions, along with other discharge data, have been employed for analysis with TRANSP.

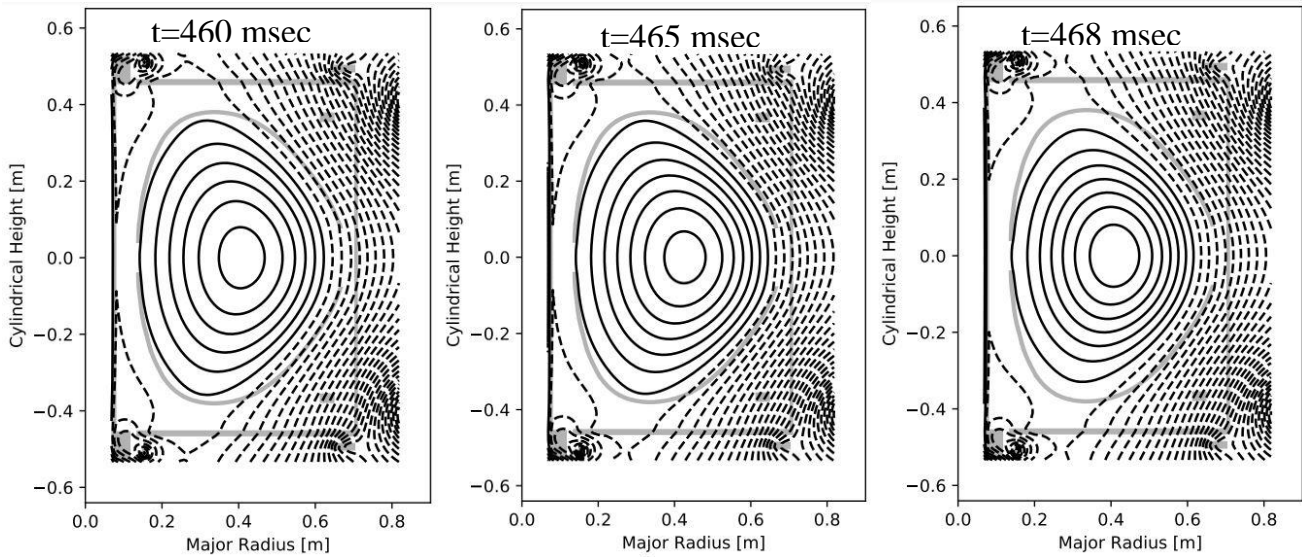


Figure 13. Psi-Tri equilibrium reconstructions during hot wall operation, constrained by the Thomson scattering temperature profiles.

Beam ion loss

Although very recently discharges have been extended to the 100 kA range of current, the upgrade of the ohmic power supply, which is part of the second DOE notable for FY20, has not been implemented. LTX-β has primarily been operating at plasma currents of 75 kA or less. At these plasma currents, the first orbit losses for the full energy component of the beam at 16 kV are very high; the first energy ions are lost before the beam ions can slow down on the plasma electron population. The first orbit losses are smaller for the half and third energy components of the beam ions. For electron temperatures in the range of 100 – 200 eV, and densities in the range of $1 \times 10^{19} \text{ m}^{-3}$, the slowing down time for fast beam ions τ_{se} on electrons is a few milliseconds. The half and third energy components are expected to slow down before they are lost through pitch angle scattering. Modeling of the beam

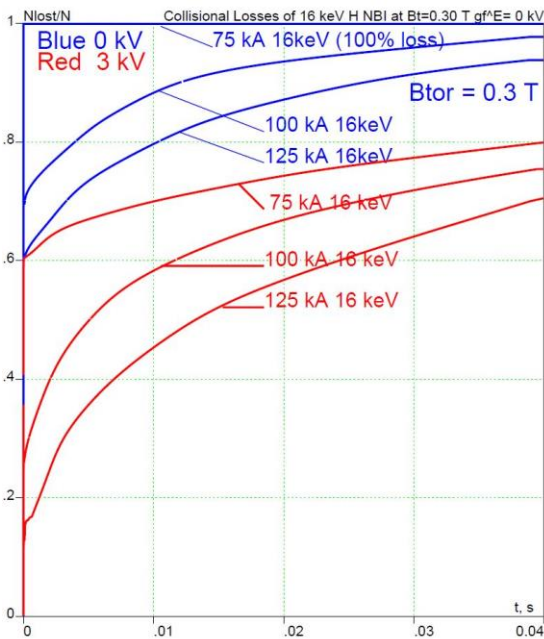


Figure 14. Beam ion losses vs. time for the full energy beam ions, for a range of plasma currents, both with, and without, a radial electric field. The calculation does not account for slowing down of beam ions on electrons, which of course would result in plasma heating by the fast ions. Losses are calculated for 16 keV injected ions, for several values of the plasma current. Losses assuming no central plasma potential are shown in blue, and losses with a central plasma potential of 3 kV are shown in red.

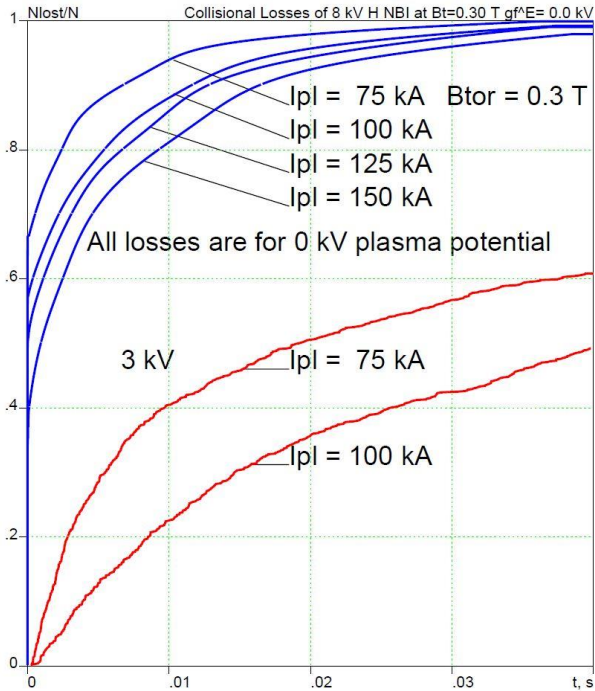


Figure 15. Beam ion losses vs. time for the half energy beam ion component, for a range of plasma currents, both with (red), and without (blue), a radial electric field, corresponding to a central plasma potential of 3 kV

ion confinement is still underway. Figure 14 shows losses of the full energy beam component as a function of time after injection, for cases with and without an electric field (due to fast ion losses). Figure 15 is the corresponding calculation for the half energy component. The calculation employed the 3DOrb code, which is fully 3D and incorporates the full LTX-β geometry (shown in Figure 16). At

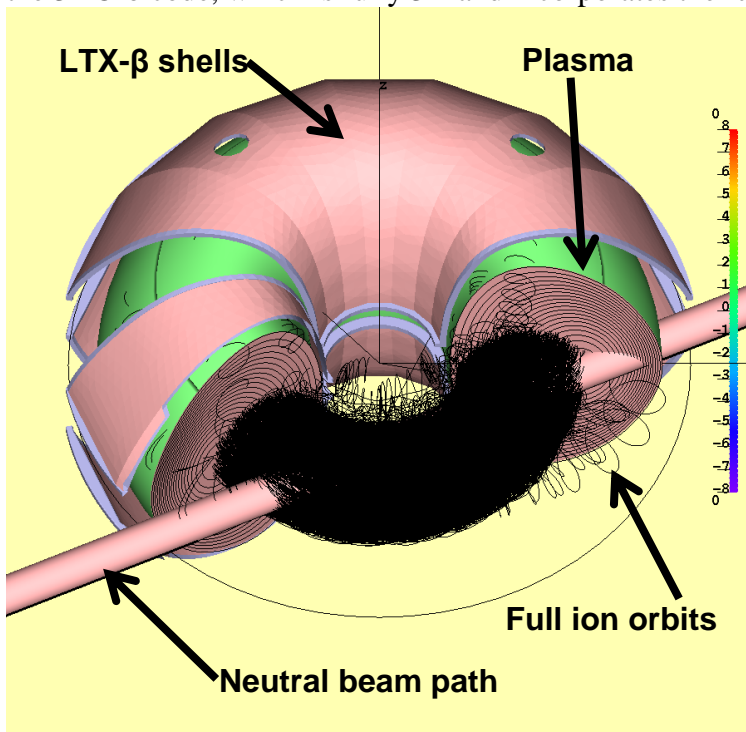


Figure 16. 3DOrb model for neutral beam injection in LTX-β. Plasma equilibrium shown here is for a 75 kA discharge.

this point 3DOrb includes pitch angle scattering only; slowing down of the fast ions by electron (or ion) drag is not yet incorporated. The electron slowing down time for these discharges is calculated to be ~2-5 msec. The development of a 3 kV plasma potential (consistent with the rotation velocity seen by the CHERS diagnostic during beam injection) would be sufficient to confine most of the half (and

third) energy beam components until they slowed down on electrons, even at low plasma current. Operation at plasma currents >100 kA should be sufficient to confine a significant fraction of fast ions at the full injection energy of 16 keV. We have also estimated beam shine-through for these discharges, which are somewhat denser than the beam target discharges developed last year. Higher density combined with lower injected beam energy has reduced shine-through to 30 - 50% for both the hot and cold wall cases.

Modeling of the fast ions, and inclusion of beam ion modeling in TRANSP, is still underway.

Energy confinement

TRANSP analysis has been performed for the hot and cold wall discharges, for which Thomson scattering is available. The TRANSP analysis assumed neoclassical ion confinement, which resulted in ion temperatures which matched the measurements from CHERS. Since only the half and third energy components of the beam ions are expected to be confined, from fast ion modeling, the beam power was NOT included in the TRANSP analysis. The results are shown in Figure 17 for hot (liquid lithium) walls, with and without beam injection.

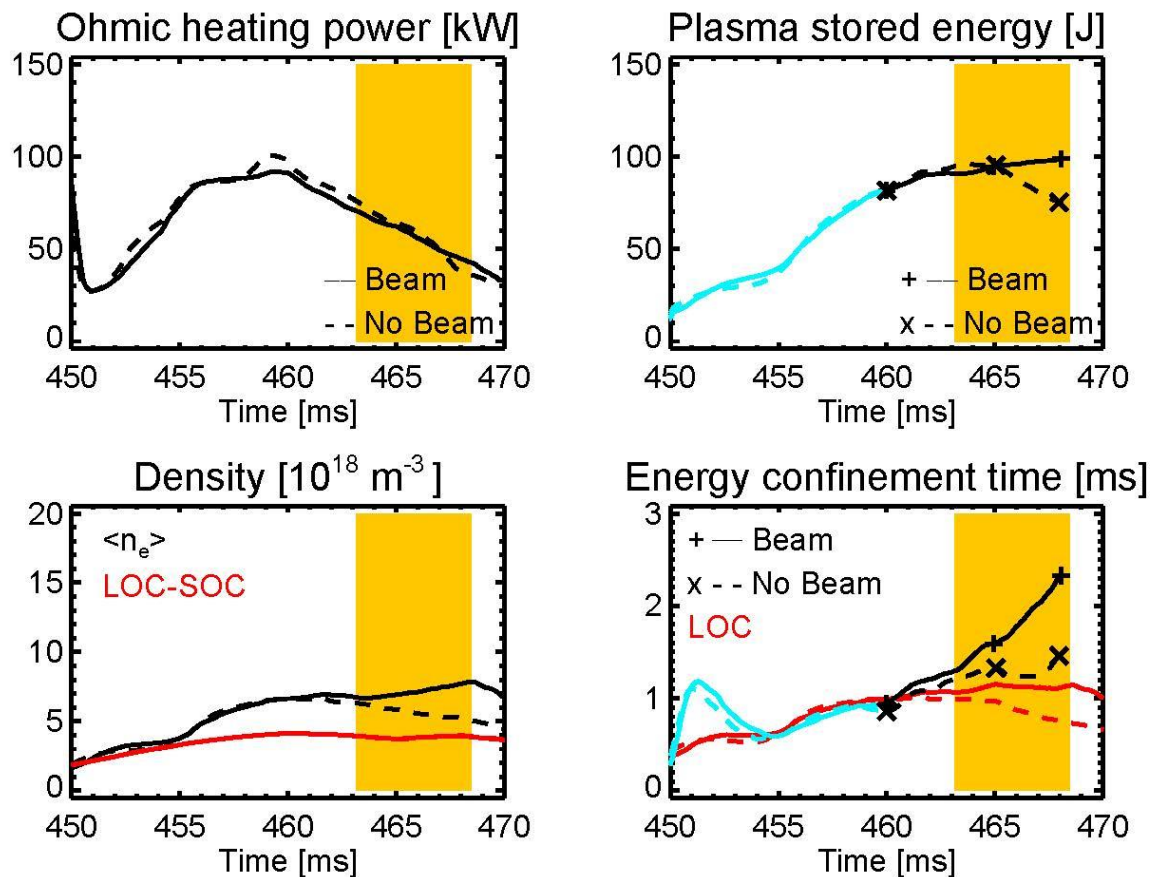


Figure 17. TRANSP analysis of the hot wall discharges – discharges with and without neutral beam injection are overlaid. Neutral beam injection was from 463 to 468 msec (yellow shaded area).

There is a modest increase in stored energy seen in the beam injected set of discharges, during injection, relative to the discharges without beam. Note that the radiated power is not available, and is set to zero in the simulations. If it is assumed that all half and third energy injected ions are completely confined, then 25 kW of additional heating power would be input from 463 to 468 msec. for the beam injected case, the energy confinement time with and without beam would be approximately equal, and would modestly exceed neo-Alcator Linear Ohmic Confinement scaling (LOC in Figures 17 and 18), later in the discharge.

Discharges with cold walls and solid lithium coatings were also analyzed with TRANSP, and are displayed in Figure 18. For the cold wall case, there is a somewhat smaller difference in the stored energy with and without the beam.

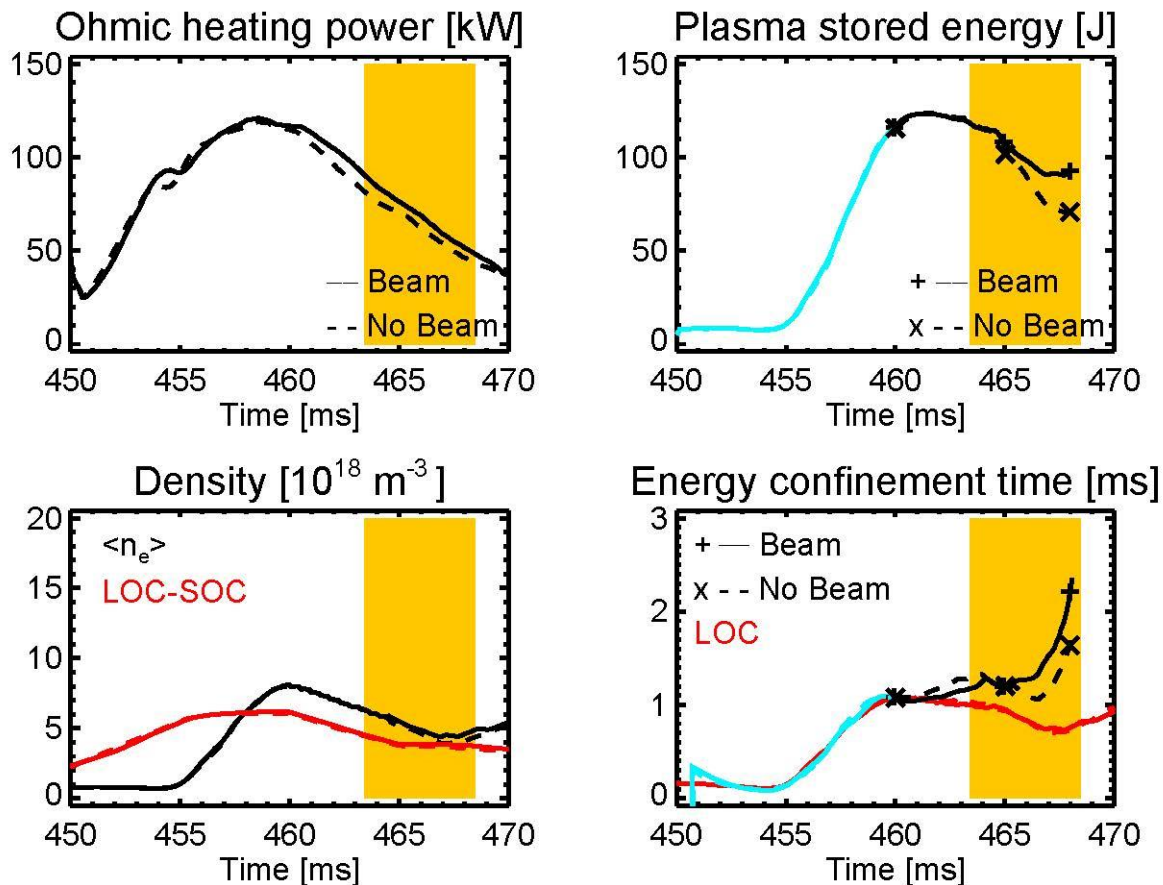


Figure 18. TRANSP analysis of the cold wall discharges, with and without NBI. Again, the time of neutral beam injection is 463 – 468 msec.

Although the effect of neutral beam injection on the cold wall discharges is less obvious, it is premature to conclude that NBI is more effective for hot walls. The set of discharges analyzed for the hot wall case was not identical to the discharges analyzed for the cold wall case, especially the fueling requirements (which evolve more strongly with hot walls and liquid lithium), and the plasma current. Continued discharge development is required for this comparison.

SUMMARY

Both Thomson scattering and active CHERS have now been commissioned on LTX- β , and operation of both diagnostics, as well as beam injection, has now been demonstrated with liquid lithium walls. The first part of the FY2020 Notable has therefore been successfully completed. However, plasma current has been limited during commissioning of these systems to 55 – 75 kA, which is not sufficient to confine the full energy component of the fast beam injected ions. In the next phase of operations, plasma current will be increased to 125 kA to improve beam ion confinement. Further, more complete accounting of fast-ion loss estimates will be included in the thermal energy confinement time analysis.